Appl Microbiol Biotechnol (2016) 100:1489–1499
DOI 10.1007/s00253-015-7085-0

BIOENERGY AND BIOFUELS

Metabolic flux analysis model for optimizing xylose conversion into ethanol by the natural C5-fermenting yeast *Candida shehatae*

Carine Bideaux[1,2,3] · **Julie Montheard**[1,2,3] · **Xavier Cameleyre**[1,2,3] · **Carole Molina-Jouve**[1,2,3] · **Sandrine Alfenore**[1,2,3]

Received: 27 February 2015 / Revised: 17 September 2015 / Accepted: 13 October 2015 / Published online: 5 November 2015

Abstract A metabolic flux analysis (MFA) model was developed to optimize the xylose conversion into ethanol using *Candida shehatae* strain. This metabolic model was compartmented and constructed with xylose as carbon substrate integrating the enzymatic duality of the first step of xylose degradation via an algebraic coefficient. The model included the pentose phosphate pathway, glycolysis, synthesis of major metabolites like ethanol, acetic acid and glycerol, the tricarboxylic acid cycle as well as the respiratory chain, the cofactor balance, and the maintenance. The biomass composition and thus production were integrated considering the major biochemical synthesis reactions from monomers to each constitutive macromolecule (i.e., proteins, lipids, polysaccharides, nucleic acids). The construction of the model resulted into a 122-linear equation system to be resolved. A first experiment allowed was to verify the accuracy of the model by comparing calculated and experimental data. The metabolic model was utilized to determine the theoretical yield taking into account oxido-reductive balance and to optimize ethanol production. The maximal theoretical yield was calculated at 0.62 $Cmol_{ethanol}/Cmol_{xylose}$ for an oxygen requirement of 0.33 $mol_{oxygen}/mol_{xylose}$ linked to the cofactors of the xylose reductase. Cultivations in chemostat mode allowed the fine tuning of both xylose and oxygen uptakes and showed that lower was the oxygen/xylose ratio, higher was the ethanol production yield. The best experimental ethanol production yield (0.51 $Cmol_{ethanol}/Cmol_{xylose}$) was obtained for an oxygen supply of 0.47 $mol_{oxygen}/mol_{xylose}$.

Keywords *Candida shehatae* metabolism · Metabolic flux analysis · Ethanol production · $Ratio_{oxygen/xylose}$

Introduction

Due to the importance of biobased alternatives for fuel substitution, ethanol from lignocellulosic biomass has been intensely studied over the last years. While the conversion of C6 sugars like glucose has been broadly mastered, C5 conversion in particular of xylose is still a scientific and technical challenge. The C5 fraction in lignocellulosic materials can represent a significant proportion in the range 10–40 % (*w*/*w*) (Singh and Mishra 1995). In order to maximize sugar conversion into ethanol, two strategies exist: one based on engineering genetically modified strains (mainly in *Saccharomyces cerevisiae*) to convert both C6 and C5 sugars and the other based on the use of naturally C5-fermenting yeasts like those of the *Pichia* or *Candida* genera.

Candida shehatae yeast has been described as a potential converter of xylose into ethanol (Toivola et al. 1984). Studies have shown that oxygen strongly impacts the capacities of the strain to produce ethanol, but its role is not entirely understood (Du Preez and van der Walt 1983; Sánchez et al. 1997). The oxygen supply affects xylose

Electronic supplementary material The online version of this article (doi:10.1007/s00253-015-7085-0) contains supplementary material, which is available to authorized users.

✉ Carine Bideaux
bideaux@insa-toulouse.fr

[1] Université de Toulouse; INSA, UPS, INP; LISBP, 135 Avenue de Rangueil, F-31077 Toulouse, France

[2] INRA, UMR792, Ingénierie des Systèmes Biologiques et des Procédés, F-31400 Toulouse, France

[3] CNRS, UMR5504, F-31400 Toulouse, France

metabolism: DuPreez et al. (1989) performed cultures with several aeration levels without any control of the dissolved oxygen concentration and showed that the xylitol production yield on xylose increased as an inverse function of the aeration. In this paper, the effect of the aeration on xylitol production was only observed between anoxic and aerobic conditions but not quantified. Interestingly, no ethanol was produced in fully aerobic culture leading to a maximal biomass production yield of 0.49 $g_{biomass}/g_{xylose}$. Controlling the dissolved oxygen tension (DOT) at 0.7 % of the air saturation, these authors obtained a maximal ethanol concentration of 45 g/L and an ethanol yield of 0.38 $g_{ethanol}/g_{xylose}$ with *C. shehatae*. More recently, Fromanger et al. (2010) quantified the oxygen limitation level by measuring the specific oxygen uptake rate in bioreactor culture of *C. shehatae* on mineral medium with xylose as substrate. They reached an ethanol yield of 0.33 $g_{ethanol}/g_{xylose}$ with 1.19 $mmolO_2/g_{DCW}/h$ and a maximal ethanol titer of 49 g/L representing 43 % of carbon consumed. The maximal yield of 0.45 $g_{ethanol}/g_{xylose}$ was obtained by Slininger et al. (1985) in flask cultures without any control of oxygen supply defined as aerobic: batch cultures in flasks were closed with perforated caps and incubated on a rotary shaker. The oxygen uptake seemed to be determinant, but optimization studies failed in the quantification of oxygen requirement and its role remains unclear. As oxygen is involved in the redox balance (Bruinenberg et al. 1983), the biological demand for cofactors of both growth and ethanol production was stringently dependent on metabolic pathways. These constraints on carbon, oxido-reductive potential, cofactors equilibrium, and energetics can be described and evaluated through metabolic models. Metabolic flux analysis (MFA) is generally used to estimate intracellular flux distribution based on a complete description of the metabolic pathways relative to substrate consumption, biomass synthesis, energy consumption and production, and metabolite production (Llaneras and Picó 2008). MFA was based on the assumption of pseudo-steady state in the intracellular concentration; it can estimate for determined/overdetermined linear systems the metabolic flux distribution without intracellular concentration measurements by fitting with measured extracellular rates such as biomass and metabolite production and substrate consumption (Stephanopoulos et al. 1998).

This paper proposes a MFA approach to understand both the role of oxygen and the carbon flux distribution of *C. shehatae* metabolism in order to define the maximal theoretical capacities of the selected yeast towards ethanol production and to optimize xylose conversion for bioethanol production. Two sets of experiments were carried out in two different culture modes in order to, first, validate to metabolic model and then to compare theoretical predicted results with experimental ones.

Material and methods

Strain and pre-culture conditions

Candida shehatae strain ATCC 22984 (American Type Culture Collection), a xylose-fermenting yeast, was maintained on plate count agar (PCA) (AES Chemunex), and its long-term storage at −80 °C used yeast extract peptone dextrose medium (YPD 10 g/L yeast extract, 10 g/L peptone, 20 g/L dextrose, and 9 g/L NaCl) adding 45 % (*v*/*v*) glycerol. Pre-cultures grown first on YPD for 24 h at 30 °C, stirred at 100 rpm, were transferred into flasks containing a complete mineral medium (Fromanger et al. 2010) complemented with 20 g/L xylose. Flask cultures were grown for 24 h at 30 °C under shaking at 100 rpm before inoculation in the bioreactor.

Medium

A mineral medium adapted to *Candida* strains was defined in order to avoid nutritional limitations up to a biomass concentration of 20 g_{CDW}/L. The pH of the medium was adjusted to 4.5, and the composition was described by Fromanger et al. (2010). To increase ethanol tolerance, a vitamin-feeding strategy was used as described by Alfenore et al. (2002) for *Saccharomyces* strains. Chemicals (xylose, salts, oligo-elements, and commercial ammonia solution) were provided from Prolabo (France) and vitamins from Sigma (France). All chemicals were of the highest analytical grade available.

Cultures in instrumented bioreactors

Two sets of experiments were carried out in two different culture modes: the data from the first were dedicated to metabolic model validation, and from the second were utilized to compare with theoretical predicted results.

The first set of experiments was performed in fed-batch mode in a 5-liter instrumented bioreactor (B Braun International Biotech, Sartorius group), with an initial working volume of 3 L. The temperature was set at 30 °C and the pH at 4.5 by addition of ammonia solution (14 % *v*/*v*). The dissolved oxygen partial pressure (pO_2) was measured by an oxygen probe (InPro® 6800 Mettler Toledo). Aeration and stirring rates were managed in order to run two different culture conditions: the first intended for growth with full oxygen supply (pO_2 up to 40 % saturation value under working conditions (30 °C, atmospheric pressure)) and the second under oxygen limitation (pO_2 of 0 % saturation) to favor ethanol production. Inlet and outlet gas compositions were monitored by mass spectrometry as described in Analytical methods and gas analysis section. The carbon substrate was supplied continuously by adding sterile xylose solution of 634 g/L.

The second set of cultivations was carried out in chemostat mode, a 2-L instrumented bioreactor (B Braun International Biotech, Sartorius group) using working volume of 1 L. Temperature and pH regulation and measurement of dissolved oxygen partial pressure were as described above for the fed-batch experiment. The substrate feeding was performed by continuously adding fresh mineral medium with a xylose concentration of 33 g/L. Three steady-state conditions were performed corresponding to different oxygen and xylose supplies and dilution rates. Details are described in the Results and Discussion sections.

Analytical methods and gas analysis

Biomass concentration was measured both by optical density and gravimetric methods. Optical density (OD) was measured at 620 nm in a spectrophotometer (Hach Lange DR 3900) in a glass cuvette (2 mm optical length) and correlated against cell dry weight measurements. Cell dry weight (CDW) was measured by filtration of a known volume through 0.45 μm-pore size polyamide membranes (Sartorius) dried at 60 °C to a constant weight under a partial vacuum (200 mmHg) for 48 h. Biomass elementary formula ($CH_xO_yN_z$) was determined at Central Analysis Service (CNRS, Solaize) on ten independent experimental samples by either combustion or pyrolysis and infrared detection or thermal conductibility.

Major fermentation products (ethanol, glycerol, xylitol, acetic acid, pyruvic acid, succinic acid, and xylose) were quantified by HPLC (Alliance 2690, Waters) in culture supernatant using an Aminex HPX 87 H column, running in isocratic mode with a flow rate of 0.5 mL/min of H_2SO_4 (5 mM) eluent, operating at 50 °C. The system was equipped with refractive index detector (RI 101—SHODEX) and UV detector (Waters 996).

Inlet and outlet gas compositions were measured by a mass spectrometer (Proline Dycor, Ametek Process Instruments) calibrated using a standard gas composition (20 % CO_2, 20 % O_2, 1 % Ar, 1000 ppm ethanol, complemented at 100 % by N_2). The volumetric O_2 consumption rate and the CO_2 production rate were calculated from mass balances involving inlet and outlet gas compositions, taking into account the evolution of the bioreactor liquid volume, the accumulation of O_2 and CO_2 in liquid and gas phases, the inlet airflow rate (regulated by a mass flow meter), and the operating temperature and pressure.

Data analysis and calculation

For each culture sample, substrate or metabolite masses produced or consumed were calculated taking into account the liquid volume variation in the bioreactor. The carbon and the oxido-reductive balances were calculated on raw data and closed at more than 90 %. Production and consumption rates were calculated using a homemade software based on polynomial regression coupled with an optimization procedure. This procedure dealt with the minimization of a quadratic criterion between the experimental and the calculated data. Moreover, the calculated rates were reconciled in order to recover all the elemental balances. Homemade software was used for metabolic flux analysis which resolved the linear equation system of metabolic fluxes with Matlab® as previously described by Bideaux et al. (2008). All the stoichiometric biochemical reactions chosen and introduced in the model were presented in the Supplementary Tables S1 to S6 (122 linear equations depended on the hypothesis formulated for the construction of the model).

Construction of the *C. shehatae* metabolic network

Candida shehatae was considered as a compartmented cell as *Saccharomyces*. So, biochemical reactions can occurr either in the cytosol or in the mitochondria, and some components can be exchanged between these two compartments as described in previous works for *Saccharomyces cerevisiae* species (Nissen et al. 1997; Pagliardini et al. 2013). Due to this fact, in the absence of specific data, the metabolic network (set of biochemical reactions) of *C. shehatae* was based on information available for *Candida utilis* strain on the database KEGG (http://www.genome.jp/kegg/kegg2.html). Compartmented model was constructed with a single carbon substrate: the xylose. Thus, the first step of xylose degradation was introduced as well as the pentose phosphate pathway, glycolysis, synthesis of major metabolites like ethanol, acetic acid, and glycerol, and the tricarboxylic acid cycle. The respiratory chain, the cofactor balance and maintenance were also included as were all the anabolic reactions (synthesis of proteins, lipids, polysaccharides, and nucleic acids linked to biomass composition and production). Each step of the construction was detailed in the further subsections.

Transport of extracellular metabolites in and out the cell was modeled through proton symports for ammonium, sulphate, and phosphate and through facilitated diffusion for the other extracellular metabolites (xylose, ethanol …) (Van Gulik and Heijnen 1995; Vanrolleghem et al. 1996).

First step of xylose degradation

As described by Bruinenberg et al. (1984), the first step of xylose degradation is performed by the enzyme xylose reductase (XR) which can be both NADH dependent and NADPH dependent. Depending on the cofactor considered for XR in the model, the redox balances in the cell were completely modified inducing different calculated intracellular fluxes to equilibrate the metabolism. To take into account both the coenzymes of XR in the metabolic model, an algebraic

coefficient called *coeffnadph* (Table 1) was introduced into the xylose degradation reaction (see Eq. 1).

This coefficient was defined as $coeffnadph = \frac{XR_{NADPH}}{XR_{NADPH}+XR_{NADH}}$.

$$\text{xylose} + coeffnadph \times \text{nadph} + (1-coeffnadph) \times \text{nadh} + \text{h} = \text{xylitol} + coeffnadph \times \text{nadp} + (1-coeffnadph) \times \text{nad} \quad (1)$$

Based on literature data relative to measured values of NADH- and NADPH-dependent XR activities (Table 2), the *coeffnadph* coefficient was within the range [0.41–0.80] depending on the culture conditions. In aerobic conditions, the mean value of the *coeffnadph* was calculated at 0.67 ± 0.05, in micro-aerobic conditions 0.6 ± 0.1, and in anoxia 0.72 ± 0.05.

Anabolism reactions

The strategy to describe the major anabolic reactions was to start from the precursors which were converted into monomers first and then into macromolecules until biomass formation. All these anabolic steps (*i.e.* from the precursors to biomass) were translated as stoichiometric equations in the model. Monomeric and macromolecular compositions in terms of lipids, proteins, polysaccharides, DNA, and RNA were initialized using data from the literature for microorganisms comparable to *C. shehatae.*

The quantities of amino acids, in mol AA/g protein, were obtained from Carnicer et al. (2009). The distribution of sterols into ergosterol, squalene, lanosterol, and obtusifoliol was determined according to Abu-Elteen and Whittaker (1997). These authors also gave a phospholipid distribution, in accordance with Rattray et al. (1975). Two groups of fatty acids were used: the palmitate group representing the fatty acids from C12:0 to C17:1 and the stearate group representing C18 fatty acid according to Thorpe and Ratledge (1972). Thus, the sterols, phospholipids and triacylglycerols accounted for 0.142, 0.532, and 0.326 g/g lipids (Abu-Elteen and Whittaker 1997). The carbohydrate content was derived from Carnicer et al. (2009): glucans and mannans each represented 42 % of the total carbohydrate fraction, glycogen 15 %, and trehalose less than 0.1 %.

Based on these data, the metabolic model was used to calculate the elementary composition of each macromolecule (proteins, lipids, carbohydrates, DNA, RNA) and compared to elementary macromolecule compositions available in the literature. Compared to data from Carnicer et al. (2009) in fully aerobic conditions for *Pichia pastoris*, the differences for $CH_xO_yN_z$ composition were obtained for proteins and lipids and were below 5 % except for N in proteins (15 %) and H and O for lipids (9 and 13 %, respectively).

In parallel, the elementary composition of biomass ($CH_xO_yN_z$) was also measured from culture samples. Then, a homemade optimization method was performed to calculate the fraction of each macromolecule in the biomass minimizing the differences between the measured elementary composition of the biomass and that calculated by the metabolic model. A set of lower and upper bounds were given for each macromolecule based on literature data analysis (Atkinson and Mavituna 1983; Carnicer et al. 2009; Castro et al. 1971; Lange and Heijnen 2001; Ratledge and Wilkinson 1988; Rattray et al. 1975). Residual water in the biomass (due to partial rehydration of samples prior to elementary analysis) was taken into account to correct the experimental measurements of the $CH_xO_yN_z$ biomass composition. The results are presented in Table 3.

Compartmentation and model construction

The model was compartmented, and reactions occurred either in the cytosol or the mitochondria as described in previous works (Nissen et al. 1997; Pagliardini et al. 2013). As proposed by Pagliardini et al. (2013, 2010), some amino acids were formed in the mitochondria (arginine, leucine, proline,

Table 1 Nomenclature

Term	Description
PPP	Pentose phosphate pathway
XR	Xylose reductase
coeffnadph	Coefficient represented the cofactor dependency of XR varying in a range [0–1]: $coeffnadph = \begin{cases} 1 \text{ if } XR \text{ only NADP Hdependent} \\ 0 \text{ if } XR \text{ only NAD Hdependent} \end{cases}$
R_i	Net extracellular rate (i = 1 to 15, respectively, for xylose, biomass, xylitol, water, pyruvic acid, acetic acid, ethanol, CO2, glycerol, O2, phosphate ions, hydrogen ions, ammonium ions, sulfate ions, and succinic acid)
r_i	Intracellular flux (i = 1 to 122). Cf. supplementary file containing the list of all the chosen reactions
$Y_{ethanol/xylose}$	Yield for xylose conversion into ethanol
$ratio_{oxygen/xylose}$	Ratio between the consumed oxygen and the consumed xylose

Table 2 Enzymatic activity of xylose reductase in *Candida shehatae* strain from the literature

C. shehatae strain	Xylose reductase (μmol.min^{-1}.mg protein^{-1})		Calculated *coeffnadph*	Condition	References
	NADH	NADPH			
CSIR Y 492	0.37	0.58	0.61	Aerobic	DuPreez et al. (1989)
	0.28	0.54	0.66	Micro-aerobic	
	0.28	0.51	0.65	Anoxic	
ATCC 22984	0.07	0.28	0.8	Aerobic	Alexander et al. (1988)
	0.08	0.31	0.79	Micro-aerobic	
	0.1	0.33	0.77	Anoxic	
CSIR Y 1632	4.93	3.4	0.41	Micro-aerobic	Yablochkova et al. (2003)
CSIR Y 1632	3.1	4.81	0.61	Aerobic	Yablochkova et al. (2004)
	4.93	3.4	0.41	Micro-aerobic	
	2.31	5.02	0.68	Anoxic	
CBS 5813	0.21	0.48	0.69	Aerobic	Bruinenberg et al. (1984)
ATCC 22984	0.3	0.48	0.62	Anoxic	Fromanger et al. (2010)
ATCC 22984	0.11	0.21	0.66	Oxygen transfer rate descending in flask cultures	Girio et al. (1989)
	0.15	0.29	0.66		
	0.13	0.26	0.67		
	0.13	0.33	0.72		
	0.1	0.23	0.68	Aerobic	
	0.14	0.35	0.71	Micro-aerobic	
	0.33	0.87	0.73	Anoxic	

valine) and others were synthesized in the cytosol. Several shuttle mechanisms were included in the model to take into account the translocation of the redox power between the different compartments.

Transport could be either direct, with some compounds easily crossing between the compartments, or more complex, via shuttles (Bruinenberg et al. 1985; Celton et al. 2012; Nissen et al. 1997). The shuttles led to substrate cycling that regenerated cytosolic NADH and increased the mitochondrial NADH pool. In this paper, one model was presented based on the ethanol-acetaldehyde shuttle (Bakker et al. 2001).

The ethanol-acetaldehyde shuttle consisted of an NADH-dependent mitochondrial alcohol dehydrogenase which converts acetaldehyde into ethanol, as these compounds can freely diffuse through the membrane.

The assumption in the model was that pyruvate, oxaloacetate, citrate, succinate, fumarate, and α-ketoglutarate can diffuse easily across the mitochondrial membrane (Granström et al. 2000). Pyruvate can be converted in the cytosol either into acetaldehyde by pyruvate decarboxylase or into oxaloacetate by pyruvate carboxylase (anaplerotic reaction) (Passoth et al. 1996). It was assumed that the pyruvate dehydrogenase was mitochondrial and catalyzed

Table 3 Elemental composition of the macromolecules of the biomass from *Candida shehatae* either calculated by the metabolic model or analyzed from cellular samples

	C	H	O	N	P	S	Calculated % *w/w* in dry biomass
Protein	1	1.57	0.35	0.3	0.01	0.0018	53.14
Carbohydrates	1	1.67	0.83	0	0	0	30.73
Lipids	1	1.85	0.14	0.0049	0.0080	0	5.3
RNA	1	1.23	0.73	0.4	0.1	0	6.54
DNA	1	1.26	0.61	0.38	0.1	0	4.29
Calculated elementary biomass composition	1	1.86	0.60	0.184	0.0145	0.001	
Analyzed elementary biomass composition	1	1.86 ± 0.03	0.60 ± 0.02	0.184 ± 0.003	0.02	0.002	

the degradation of pyruvate into acetyl-coA (Granström et al. 2000). The NAD^+-dependent acetaldehyde dehydrogenase was assumed to be cytosolic as was the $NADP^+$-dependent isocitrate dehydrogenase (Bruinenberg et al. 1985) to replenish the NADPH stock in this compartment. Cytosolic acetate participated in acetyl-CoA synthesis in the cytosol via acetyl-CoA synthetase. This compound is involved in sterol and fatty acid synthesis. ATP consumption for maintenance energy and pH homeostasis were also included according to Van Gulik and Heijnen (1995). The oxidative phosphorylation coefficient (PO) was fixed at 1.33 for both NADH and FADH oxidation according to Verduyn et al. (1991).

As a conclusion, the stoichiometric matrix ($n \times m$) construction resulted in a system containing $n = 137$ metabolites and $m = 122$ intracellular rates (Supplementary Tables S1 to S6), and the retained metabolic network was summarized in Fig. 1. Net rates of 15 extracellular compounds were considered: xylose, biomass, xylitol, water, pyruvic acid, acetic acid, ethanol, CO_2, glycerol, O_2, phosphate ions, hydrogen ions, ammonium ions, sulfate ions, and succinic acid (noted from R1 to R15, Supplementary Table S2). The degree of freedom for the model was 8, meaning that a least eight independent net rates had to be measured to calculate a single solution for each system.

Results

The stoichiometric model developed was validated using experimental data. The dynamic behavior of *C. shehatae* during growth and ethanol production was characterized during a fed-batch culture with xylose as carbon source. The culture was carried out in two phases: growth only and both growth and ethanol production. The produced metabolites or consumed substrate were plotted in mass in Fig. 2. The first phase was dedicated to growth in aerobic conditions (dissolved oxygen pressure (pO_2) up to 40 % of saturation value). This phase allowed reaching a biomass concentration close to 50 g/L in 50 h of culture. The second phase, dedicated to both biomass and ethanol production, was monitored under oxygen limitation (i.e. oxygen was supplied by aeration below the oxygen requirement of the biomass, and pO_2 was below detection limit and considered as nil). During the next 30 h, culture biomass concentration reached nearly 65 g_{CDW}/L whereas

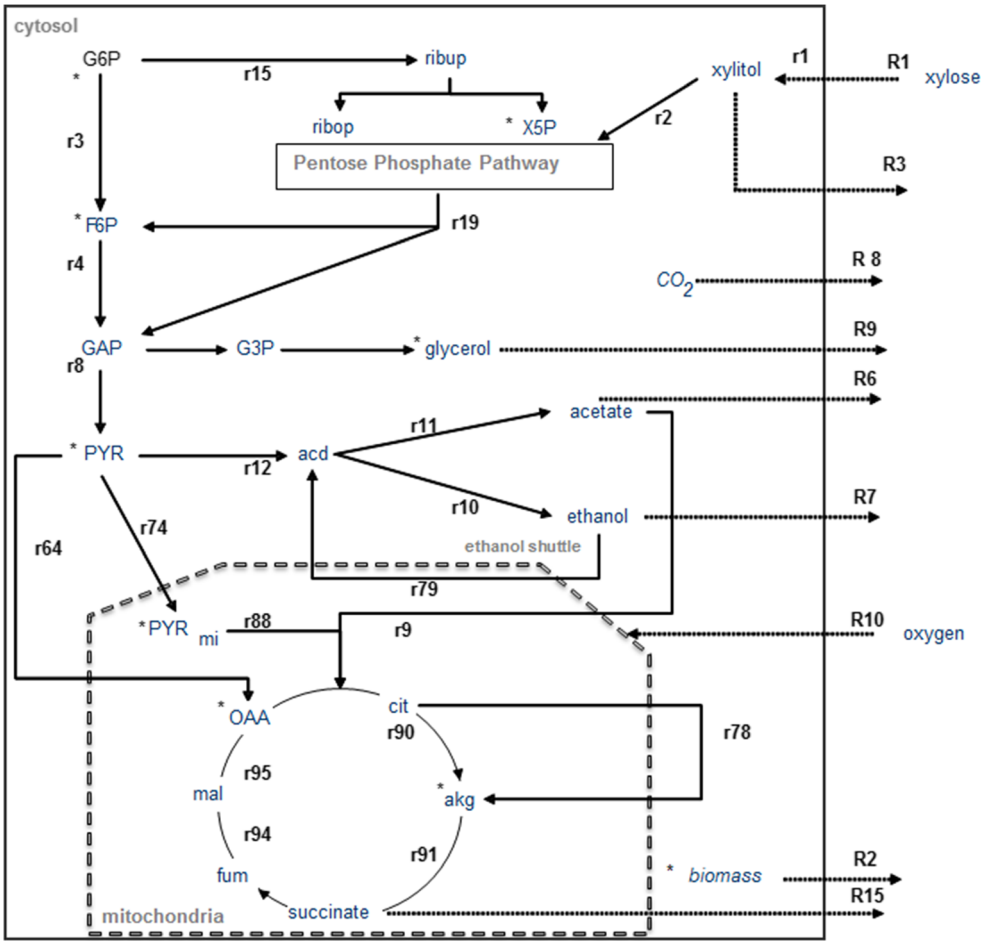

Fig. 1 Representation of the chosen metabolic network of *Candida shehatae*. r_i intracellular flux, R_i net extracellular rate

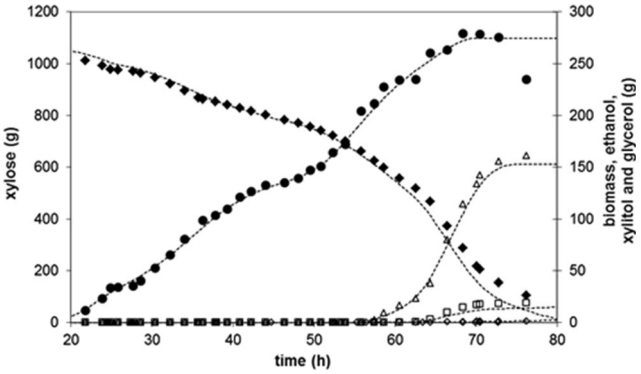

Fig. 2 Evolution of substrate and product masses during the validation experiment. Experimental values for (*filled diamond*) xylose (g), (*filled circle*) biomass (g), (*empty triange*) ethanol (g), (*empty square*) xylitol (g), (*empty diamond*) glycerol (g)—reconciliated values in *dashed lines*

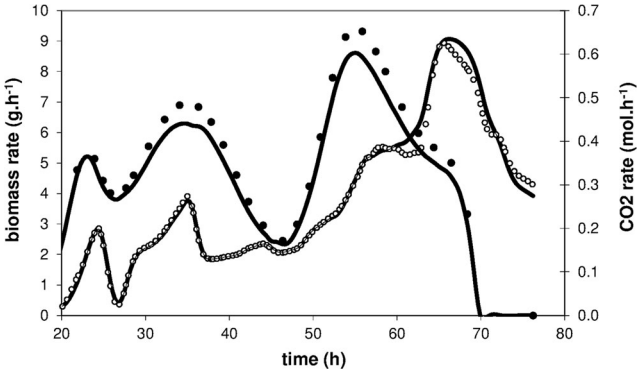

Fig. 3 Comparison of experimental rates for biomass (*filled circle*) and CO_2 (*empty circle*) compared to those calculated by the model (*full lines*)

ethanol production was close to 35 g/L. Low xylitol production was observed representing less than 3 % of the carbon consumed. Carbon and oxido-reductive balances were recovered at 97.6 and 99.1 %, respectively.

The maximal specific growth rate of 0.43 h^{-1} was obtained. The average biomass yield was 0.49 $g_{biomass}/g_{xylose}$ (*i.e.*, 96 % of the theoretical yield). During this phase, both ethanol and biomass were produced with global yields of 0.10 and 0.20 $g_{ethanol}/g_{xylose}$, respectively. The instantaneous maximal ethanol yield reached 0.35 $g_{ethanol}/g_{xylose}$. All the rates (expressed in g/h or mol/h) were calculated for ethanol, xylitol, biomass, organic acids, CO_2, and glycerol productions and for both xylose and O_2 consumptions to be used to validate the proposed metabolic model.

Validation of the metabolic models

Model calculations were validated by comparing experimental and calculated rates. Based on experimental measurements, ten net rates were determined during culture and eight of them were supplied to the metabolic model for resolution. Validation used the two other extracellular rates. As biomass and CO_2 were the major products in the two phases (99 and 65 % of the total consumed carbon during the aerobic and the oxygen limited phases, respectively), these two metabolite rates were chosen for error estimation. As the culture was carried out in aerobic conditions with a controlled value of the specific oxygen consumption rate (not null), the value of *coeffnadph* was fixed at 0.67 according to literature data reported in Table 2. Figure 3 overlaid both the calculated and the experimental rates for the metabolites as a function of time. The calculated rates were close to the experimental ones with average quadratic discrepancies of 3.5 and 0.1 % for biomass and CO_2 rates, respectively. As the average discrepancies for calculated biomass and CO_2 rates were quite low, the model was considered valid; it is suitable to correctly describe the metabolism of *C. shehatae*.

Utilization of the model to determine the theoretical maximal ethanol yield

The ethanol-acetaldehyde shuttle model was used to calculate the maximal theoretical yield for xylose conversion into ethanol only. For mathematical resolution, the consumption rate of xylose was set at −100 mol/h and the production rates for biomass and other co-metabolites (xylitol, glycerol, pyruvic, acetic, and succinic acid rates) were set at 0. Oxygen rate varied between 0 and 2.6 mol/h. Based on these constraints, both CO_2 and ethanol rates were calculated.

Based on thermodynamic or enzymatic constraints, some reactions were defined as irreversible: the oxidative part of the PPP and the pyruvate dehydrogenase reaction. These reactions were cofactors dependent and then impacted by oxygen and had to be either nil or positive. Depending on the values of the *coeffnadph*, lower and upper bounds were found for the ratio oxygen/xylose to satisfy this criterion. The space was then reduced to the sole possible biological solutions. This was traduced as a dark grey triangle on Fig. 4, whereas all the excluded solutions appeared in the light grey areas. Regarding the equation of the global plan (both light and dark grey areas), the theoretical ethanol yield was not directly impacted by the value of *coeffnadph* and was assumed to be dependent on the ratio oxygen/xylose only (Eq. 2).

$$Y_{ethanol/xylose} = -4.550.10^{-16} \times coeffnadph - 0.133 \times ratio_{oxygen/xylose} + 0.667 \quad (2)$$

Thus, Eq. 2 can be simplified as Eq. 3.

$$Y_{ethanol/xylose} = -0.133 \times ratio_{oxygen/xylose} + 0.667 \quad (3)$$

As already mentioned, the value of *coeffnadph* reduced the space of the possible biological solutions for the oxygen/

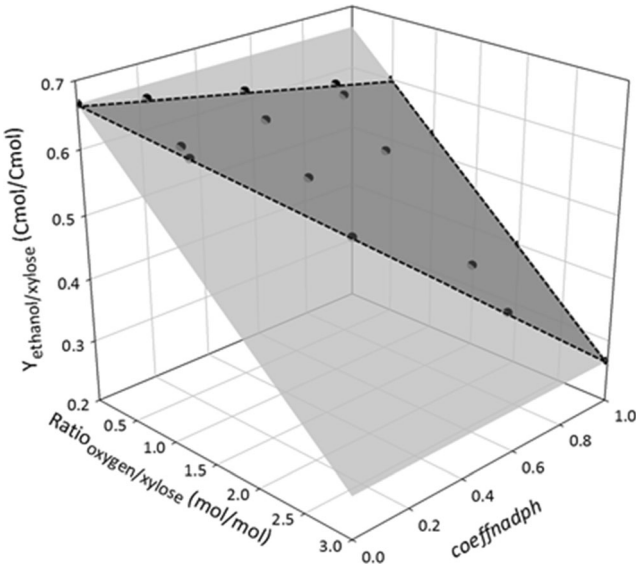

Fig. 4 Space of solutions for theoretical ethanol yield as a function of both the $ratio_{oxygen/xylose}$ and *coeffnadph*. Thermodynamically possible biological solutions are in the *dark grey triangle*, whereas all the excluded solutions appeared in the *light grey areas*

xylose ratio. For a *coeffnadph* value fixed at 0.67 (i.e., for fully aerobic culture conditions), the model resolution gave a range of between 0.33 and 2 $mol_{oxygen}/mol_{xylose}$ for possible oxygen/xylose ratio ($ratio_{oxygen/xylose}$). A value for $ratio_{oxygen/xylose}$ of 0.33 mol/mol corresponded to an inlet flux in the TCA cycle equal to 0 which meant no growth and all the carbon flux converted into ethanol production. For $ratio_{oxygen/xylose}$ values higher than 2 $mol_{oxygen}/mol_{xylose}$, the oxidative part of the PPP became negative.

As the critical value for oxygen/xylose ratio was 0.33 $mol_{oxygen}/mol_{xylose}$, the equation found (Eq. 3) allowed the calculation of a maximal theoretical ethanol yield of 0.62 $Cmol_{ethanol}/Cmol_{xylose}$ (*i.e.* 0.475 $g_{ethanol}/g_{xylose}$).

Optimizing the conversion of xylose into ethanol in chemostat

Based on the correlation found between $ratio_{oxygen/xylose}$ and $Y_{ethanol/xylose}$ (Eq. 3), the next strategy was to control different $ratio_{oxygen/xylose}$ in a range between 0.33 and 2 $mol_{oxygen}/mol_{xylose}$ in a chemostat culture to experimentally quantify its effect on the ethanol yield. The chemostat culture was carried out in oxido-reductive mode, *i.e.*, with a necessary part of biomass production (and thus the resulting ethanol yield was lower than the expected theoretical one which was calculated under reductive hypothesis without any other co-production except CO_2). All the culture conditions and results are detailed in Table 4. For each steady state, both the carbon and oxido-reductive balances were closed to 97 %. Three dilution rates were carried out in aerated conditions under oxygen limitation (pO2 = 0, *i.e.* pO_2 below detection limit). The results showed that decreasing the $ratio_{oxygen/xylose}$ led to a minimization of the biomass and byproducts production to 13 % of the total carbon consumed (see steady state 1). In this culture condition ($ratio_{oxygen/xylose}$ = 0.47 $mol_{oxygen}/mol_{xylose}$), the ethanol yield (0.51 $Cmol_{ethanol}/Cmol_{xylose}$) corresponded to 85 % of the expected maximal theoretical ethanol yield (*i.e.* 0.60 Cmol/Cmol). Figure 5 shows the experimental ethanol yields obtained for each steady state in comparison with the maximal theoretical ethanol yields calculated by the metabolic model in strictly reductive conditions (*i.e.* only CO_2 and ethanol production).

$Y_{ethanol/xylose}$ increased as $ratio_{oxygen/xylose}$ decreased as predicted by the model. The flux through the TCA cycle (r88) decreased and the carbon flux was directed from the biomass to ethanol. $Y_{ethanol/xylose}$ in the three steady states attained 50, 72, and 85 % of $Y_{ethanol/xylose}$ calculated, respectively. In oxido-reductive conditions, mainly producing biomass, ethanol and CO_2, a linear correlation between the experimental $Y_{ethanol/xylose}$ and $ratio_{oxygen/xylose}$ was found (Eq. 4) with a high value of R^2 (0.9997):

$$Y_{ethanol/xylose} = -0.3027 \times ratio_{oxygen/xylose} + 0.6524 \quad (4)$$

In chemostat culture conditions for $ratio_{oxygen/xylose}$ equal to 0.33 mol/mol, the calculated maximal ethanol yield would be 0.55 $Cmol_{ethanol}/Cmol_{xylose}$, *i.e.* 88 % of the theoretical yield in fully reductive mode. The residual part of the carbon was due to biomass formation which occurred under these oxido-reductive culture conditions.

Discussion

In this work, a compartmented model was constructed for *Candida shehatae* species with xylose as the sole carbon substrate. Three previous works were found in the literature relative to metabolic models for *Candida* genus or *Pichia* genus which was phylogenetically close to *Candida*. Two MFA models were proposed by Granström et al (2002; 2000) dealing with *Candida* species growing on both glucose and xylose or glucose, xylose, and formate, whereas the third one concerned *Pichia stipitis* growing on both glucose and xylose (Unrean and Nguyen 2012) using elementary flux modes analysis. For Granström et al. (2000) and Unrean and Nguyen (2012), the xylose reductase activity was strictly NADPH dependent and the biomass was generated either from macromolecules (Granström et al. 2000) or by both nine precursors, cofactors, ammonia, and ATP (Unrean and Nguyen 2012). In 2002, Granström et al. (2002) modified their first model including a variable coefficient for XR activity; the biomass description remained as in the previous work.

The proposed metabolic network for *Candida shehatae* was defined as stoichiometric reactions dealing with the first

Table 4 Main characteristics of the chemostat experiment

	Steady state 1	Steady state 2	Steady state 3
Dilution rates (h^{-1})	0.039 ± 0.006	0.039 ± 0.007	0.09 ± 0.01
q_S ($mmol_{xylose}.g_X.h^{-1}$)	3.95 ± 0.04	2.037 ± 0.002	2.61 ± 0.01
q_{O2} ($mmol_{oxygen}.g_X.h^{-1}$)	1.86 ± 0.03	1.696 ± 0.004	3.52 ± 0.01
$Y_{oxygen/xylose}$ ($mol.mol^{-1}$)	0.47 ± 0.03	0.83 ± 0.01	1.35 ± 0.05
$Y_{ethanol/xylose}$ ($Cmol.Cmol^{-1}$)	0.512 ± 0.001	0.397 ± 0.001	0.245 ± 0.002
$Y_{biomass/xylose}$ ($Cmol.Cmol^{-1}$)	0.103 ± 0.001	0.197 ± 0.001	0.28 ± 0.04
$Y_{CO2/xylose}$ ($Cmol.Cmol^{-1}$)	0.358 ± 0.001	0.3797 ± 0.0003	0.413 ± 0.004
$Y_{acids/xylose}$ ($Cmol.Cmol^{-1}$)	0.003 ± 0.001	0.0010 ± 0.0004	0.019 ± 0.006
$Y_{(xylitol + glycerol)/xylose}$ ($Cmol.Cmol^{-1}$)	0.024 ± 0.003	0.024 ± 0.002	0.044 ± 0.001

step of xylose degradation, the pentose phosphate pathway, glycolysis, synthesis of major metabolites like ethanol, acetic acid and glycerol, and the tricarboxylic acid cycle. The respiratory chain and the cofactor balance and maintenance were also included as were all the anabolic reactions (synthesis of proteins, lipids, polysaccharides, and nucleic acids linked to biomass composition and production).

Based on the experimental elementary composition of biomass ($CH_xO_yN_z$) and using a homemade optimization method, the fraction of each macromolecule in the biomass was calculated minimizing the differences between the measured elementary composition of the biomass and the calculated one (Table 3).

The calculated protein percentage in dry biomass was 53 % close to the value obtained by Granström et al. (2002; 2000) (protein content of 52 % for *Candida tropicalis* on xylose). The results of Carnicer et al. (2009) were between 35 and 41 % for *Pichia pastoris* strain depending on the analysis method (Lowry's quantification or amino acid measurements) and proteins reached 37 % after their own reconciliation procedure. Carbohydrates represented 37 % of biomass for Carnicer et al. (2009) after their reconciliation procedure, 42 % for Granström et al. (2002; 2000), while the value calculated here was

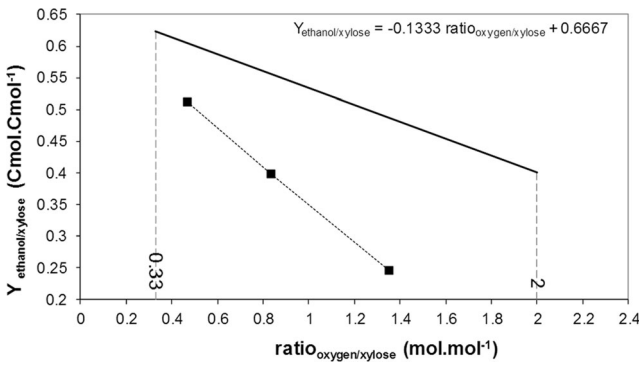

Fig. 5 Comparison of theoretical ethanol yield and experimental ethanol yield obtained for cultures in chemostat mode as a function of the $ratio_{oxygen/xylose}$. The yields obtained in steady state are plotted in *solid squares* and the theoretical relationship as a *line*. The limits of thermodynamical validity of the model are plotted by *dashed lines*

significantly lower (30.7 %). The lipid content was calculated at 5.3 %, whereas Carnicer et al. (2009) obtained 6.2 % and Granström et al. (2002; 2000) reached 3 % corresponding to the sum of both oleate and palmitoleate groups. For Rattray et al. (1975), the lipid contents were qualified as weak for *C. utilis* (<5 % cell dry weight) and middle (5 to 15 %) for *C. tropicalis*. For RNA content, Granström et al. (2002; 2000) found 6.3 % whereas Carnicer et al. (2009) found 6.6 %. The value obtained was 6.5 % in this study in accordance with the previous literature data. The calculated DNA content was at a the value of 4.3 % which was very different from those obtained by Carnicer et al. (2009), (0.13 %), whereas Granström et al. (2002; 2000) did not assess the DNA. Water content was found at 8.5 % (*w*/*w*) (Carnicer et al. 2009 for *Pichia stipitis* (6.3 %). Moreover, Carnicer et al. (2009) included in their biomass composition a part of sulfate and metals which both represented 6.9 % of the calculated biomass composition. These components were neglected in this work.

The coefficient *coeffnadph* was introduced to represent the dependence of the XR on two cofactors NADH and NADPH as proposed by Granström et al. (2002). It can be adjusted between 0 and 1 to traduce the metabolic flexibility of the strain under various oxygen conditions (full aerobiosis, oxygen limitation, or anoxia). A sensitivity analysis was carried out to evaluate the impact of the variation of this parameter on the results of the calculation of intracellular flux distribution (data not shown). The highest impacts were obtained on the fluxes involving in the biomass synthesis mainly for fluxes dealing with phosphoglucose isomerase (noted r3) and ribulose-5-phosphate isomerase (noted r16), the transport of some compounds across the mitochondrial membrane in association with cytosolic isocitrate dehydrogenase (r78; r73; r77), the TCA cycle (r91→r95), the reduction of $FADH_2$ in the respiratory chain (r98), and the oxidative part of the pentose phosphate pathway (PPP) (noted r15).

Concerning theoretical ethanol production yields (*i.e.* model used in reductive conditions with only ethanol and CO_2 productions), the variation of the value of *coeffnadph* allowed

defining lower and upper bounds for the $ratio_{oxygen/xylose}$ to satisfy all the thermodynamic constraints reducing the space of the possible biological solutions. In these defined area, the variation of *coeffnadph* had no effect on theoretical ethanol yields, so it was then possible to write a linear correlation between this yield and the $ratio_{oxygen/xylose}$. This result was in accordance with Unrean and Nguyen (2012) works which showed that the decrease of $ratio_{oxygen/xylose}$ led to an increase in $Y_{ethanol/xylose}$ using elementary flux modes analysis (Unrean and Nguyen (2012)). The obtained linear correlation permitted to calculate the range for the theoretical ethanol yield between 0.62 and 0.40 $Cmol_{ethanol}/Cmol_{xylose}$ when the ratio oxygen/xylose varied from 0.33 to 2 $mol_{oxygen}/mol_{xylose}$. In accordance, an ethanol yield of 0.62 $Cmol_{ethanol}/Cmol_{xylose}$ (*i.e.* 0.475 $g_{ethanol}/g_{xylose}$) was suggested by Evans and Ratledge (1984) in various xylose consuming yeasts assuming that 15 % of xylose was recycled to provide NADPH for ethanol production.

The proposed metabolic model was validated on fed-batch cultures of *Candida shehatae* comparing experimental and calculated extracellular rates for biomass and CO_2 production rates (discrepancies of 5.1 and 1.0 % for biomass and CO_2 rates, respectively). In this experiment, the aerobic phase was dedicated to growth only with a maximal specific growth rate of 0.43 h^{-1} which is similar to that obtained by Fromanger et al. (2010). The average biomass yield was 0.49 $g_{biomass}/g_{xylose}$ (*i.e.* 96 % of the theoretical yield) according to Du Preez et al. (1989). During the second phase, both ethanol and biomass were produced with global yields of 0.10 $g_{biomass}/g_{xylose}$ and 0.20 $g_{ethanol}/g_{xylose}$. The instantaneous maximal ethanol yield reached 0.35 g/g, which was lower than the maximal yield obtained by Slininger et al. (1985), *i.e.* 0.45 g/g in aerobic flask cultures.

A metabolic model was successfully developed on *Candida shehatae* for the description of xylose metabolism. A coefficient *coeffnadph* was included in the metabolic model to represent the dependence of the XR on two cofactors in the metabolic model. The network structure was validated on experimental data (discrepancy <3.5 %). The model resolution gave a range between 0.33 and 2 $mol_{oxygen}/mol_{xylose}$ for $ratio_{oxygen/xylose}$ for pure conversion of xylose into ethanol and a linear correlation was obtained indicating that higher was the ethanol yield as lower was the ratio between consumed oxygen and consumed xylose. Based on simulations, an ethanol yield of 0.51 $Cmol_{ethanol}/Cmol_{xylose}$ (*i.e.* 85 % of the maximal ethanol yield) was obtained in chemostat cultures for a $ratio_{oxygen/xylose}$ of 0.47 $mol_{oxygen}/mol_{xylose}$ controlling both the oxygen and xylose uptakes. This result is in accordance with theoretical results, showing the relevance of the model to describe the xylose metabolism of *Candida shehatae* and to propose innovative culture strategies to optimize the ethanol production yield on xylose with by product minimization.

Acknowledgments This work was carried out as part of the FUTUROLPROJECT, and the authors want to thank OSEO Innovation for its financial support and Dr. P. Winterton for the help in preparing the English manuscript.

Compliance with ethical standards All the authors declare that there is no potential conflict of interest (financial or non-financial), and that this research work did involve neither human participants nor animals.

References

Abu-Elteen K, Whittaker P (1997) Effect of sub-inhibitory concentration of chlorhexidine on lipid and sterol composition of shape *Candida albicans*. Mycopathol 140:69–76

Alexander MA, Yang VW, Jeffries TW (1988) Levels of pentose phosphate pathway enzymes from *Candida shehatae* grown in continuous culture. Appl Microbiol Biotechnol 29:282–288

Alfenore S, Molina-Jouve C, Guillouet SE, Uribelarrea JL, Goma G, Benbadis L (2002) Improving ethanol production and viability of *Saccharomyces cerevisiae* by a vitamin feeding strategy during fed-batch process. Appl Microbiol Biotechnol 60:67–72

Atkinson B, Mavituna F (1983) Biochemical engineering and biotechnology handbook vol 1. Trends in Biotechnology, vol 3. Macmillan Publishers Ltd,

Bakker BM, Overkamp KM, van Maris AJA, Kötter P, Luttik MAH, van Dijken JP, Pronk JT (2001) Stoichiometry and compartmentation of NADH metabolism in *Saccharomyces cerevisiae*. FEMS Microbiol Rev 25:15–37

Bideaux C, Goma G, Uribelarrea J-L, Dahhou B, Roux G (2008) Stoichiometric modelling approach for microbial cultures monitoring. Int J Model Identif Control 3:413–426

Bruinenberg PM, Bot PHM, Dijken JP, Scheffers WA (1983) The role of redox balances in the anaerobic fermentation of xylose by yeasts. Appl Microbiol Biotechnol 18:287–292

Bruinenberg PM, Bot PHM, Dijken JP, Scheffers WA (1984) NADH-linked aldose reductase: the key to anaerobic alcoholic fermentation of xylose by yeasts. Appl Microbiol Biotechnol 19:256–260

Bruinenberg PM, Van Dijken JP, Gijs Kuenen J, Scheffers WA (1985) Oxidation of NADH and NADPH by mitochondria from the yeast *Candida utilis*. J Gen Microbiol 131:1043–1051

Carnicer M, Baumann K, Toplitz I, Sanchez-Ferrando F, Mattanovich D, Ferrer P, Albiol J (2009) Macromolecular and elemental composition analysis and extracellular metabolite balances of *Pichia pastoris* growing at different oxygen levels. Microb Cell Factories 8:65–79

Castro AC, Sinskey AJ, Tannenbaum SR (1971) Reduction of nucleic acid content in *Candida* yeast cells by bovine pancreatic ribonuclease A treatment. Appl Microbiol 22:422–427

Celton M, Goelzer A, Camarasa C, Fromion V, Dequin S (2012) A constraint-based model analysis of the metabolic consequences of increased NADPH oxidation in *Saccharomyces cerevisiae*. Metab Eng 14:366–379

Du Preez JC, Driessel B, Prior BA (1989) Effect of aerobiosis on fermentation and key enzyme levels during growth of *Pichia stipitis*, *Candida shehatae* and *Candida tenuis* on D-xylose. Arch Microbiol 152:143–147

Du Preez JC, van der Walt JP (1983) Fermentation of D-xylose to ethanol by a strain of *Candida shehatae*. Biotechnol Lett 5:357–362

DuPreez JC, Driessel B, Prior BA (1989) Ethanol tolerance of *Pichia stipitis* and *Candida shehatae* strains in fed-batch cultures at controlled low dissolved oxygen levels. Appl Microbiol Biotechnol 30: 53–58

Evans C, Ratledge C (1984) Induction of xylulose-5-phosphate phosphoketolase in a variety of yeasts grown on D-xylose: the key to efficient xylose metabolism. Arch Microbiol 139:48–52

Fromanger R, Guillouet SE, Uribelarrea JL, Molina-Jouve C, Cameleyre X (2010) Effect of controlled oxygen limitation on *Candida shehatae* physiology for ethanol production from xylose and glucose. Journal of Industrial Microbiology & Biotechnology 37:437–445

Girio FM, Peito MA, Amaral-Collaco MT (1989) Enzymatic and physiological study of D-xylose metabolism by *Candida shehatae*. Appl Microbiol Biotechnol 32:199–204

Granström T, Aristidou AA, Leisola M (2002) Metabolic flux analysis of *Candida tropicalis* growing on xylose in an oxygen-limited chemostat. Metab Eng 4:248–256

Granström TB, Aristidou AA, Jokela J, Leisola M (2000) Growth characteristics and metabolic flux analysis of *Candida milleri*. Biotechnol Bioeng 70:197–207

Lange HC, Heijnen JJ (2001) Statistical reconciliation of elemental and molecular biomass composition of *Saccharomyces cerevisiae*. Biotechnol Bioeng 75:334–344

Llaneras F, Picó J (2008) Stoichiometric modelling of cell metabolism. J Biosci Bioeng 105:1–11

Nissen TL, Schulze U, Nielsen J, Villadsen J (1997) Flux distributions in anaerobic, glucose-limited continuous cultures of *Saccharomyces cerevisiae*. Microbiol 143:203–218

Pagliardini J, Hubmann G, Alfenore S, Nevoigt E, Bideaux C, Guillouet SE (2013) The metabolic costs of improving ethanol yield by reducing glycerol formation capacity under anaerobic conditions in *Saccharomyces cerevisiae*. Microb Cell Factories 12:29

Pagliardini J, Hubmann G, Bideaux C, Alfenore S, Nevoigt E, Guillouet S (2010) Quantitative evaluation of yeast's requirement for glycerol formation in very high ethanol performance fed-batch process. Microb Cell Factories 9:36

Passoth V, Zimmermann M, Klinner U (1996) Peculiarities of the regulation of fermentation and respiration in the crabtree-negative, xylose-fermenting yeast *Pichia stipitis*. Appl Biochem Biotechnol 57-8:201–212

Ratledge C, Wilkinson SG (1988) Microbial lipids. Academic Press, London

Rattray JB, Schibeci A, Kidby DK (1975) Lipids of yeasts. Bacteriol Rev 39:197–231

Sánchez S, Bravo V, Castro E, Moya AJ, Camacho F (1997) The influence of pH and aeration rate on the fermentation of xylose by *Candida shehatae*. Enzym Microb Technol 21:355–360

Singh A, Mishra P (1995) Microbial pentose utilization: current applications in biotechnology. Elsevier Science

Slininger PJ, Bothast RJ, Okos MR, Ladisch MR (1985) Comparative evaluation of ethanol production by xylose fermenting yeasts presented high xylose concentrations. Biotechnol Lett 7:431–436

Stephanopoulos G, Aristidou A, Nielsen J (1998) Metabolic engineering: principles and methodologies, 1st edn. Academic Press, San Diego

Thorpe RF, Ratledge C (1972) Fatty acid distribution in triglycerides of yeasts grown on glucose or n-alkanes. J Gen Microbiol 72:151–163. doi:10.1099/00221287-72-1-151

Toivola A, Yarrow D, Van Den Bosch E, Van Dijken JP, Scheffers WA (1984) Alcoholic fermentation of D-xylose by yeasts. Appl Environ Microbiol 47:1221–1223

Unrean P, Nguyen NA (2012) Metabolic pathway analysis of *Scheffersomyces* (*Pichia*) *stipitis*: effect of oxygen availability on ethanol synthesis and flux distributions. Appl Microbiol Biotechnol 94:1387–1398

Van Gulik WM, Heijnen JJ (1995) A metabolic network stoichiometry analysis of microbial growth and product formation. Biotechnol Bioeng 48:681–698

Vanrolleghem PA, de Jong-Gubbels P, van Gulik WM, Pronk JT, van Dijken JP, Heijnen S (1996) Validation of a metabolic network for *Saccharomyces cerevisiae* using mixed substrate studies. Biotechnol Prog 12:434–448. doi:10.1021/bp960022i

Verduyn C, Stouthamer AH, Scheffers WA, Van Dijken JP (1991) A theoretical evaluation of growth yields of yeasts. Antonie Van Leeuwenhoek 59:49–63

Yablochkova EN, Bolotnikova OI, Mikhailova NP, Nemova NN, Ginak AI (2003) The activity or xylose reductase and xylitol dehydrogenase in yeasts. Microbiol 72:414–417

Yablochkova EN, Bolotnikova OI, Mikhailova NP, Nemova NN, Ginak AI (2004) The activity of key enzymes in xylose-assimilating yeasts at different rates of oxygen transfer to fermentation medium. Microbiol 73:129–133